



Disinfection with UV-A and UV-B sunlight by concentration

G. Bonanno, G. Romeo, G. Occhipinti

Istituto Nazionale di Astrofisica – Osservatorio Astrofisico di Catania, Via S. Sofia 78, I-95123 Catania, Italy
e-mail: giovanni.bonanno@inaf.it

Received: 9 October 2021; Accepted: 3 May 2022

Abstract. It has recently been shown that UV radiation appears to have a stronger than expected effect on the inactivation of viruses and bacteria. And in the case of UV-C radiation, a dose of about 4 mJ/cm^2 is enough to obtain a virucidal effect of about 99%. In the case of UV-B radiation, a dose of about 50 times higher is required to obtain the same effect and in the case of UV-A the required dose must be approximately 1000 times higher than that of UV-C radiation. A solution to increase solar radiation in a certain position is certainly to use a solar concentrator or mirror, a more complex and expensive system that is not easy to manage, or a Fresnel lens, a simpler and easier system to implement. This last, by reducing the active area, can increase the power collected in the focal plane by 50 or 100 times. This article describes the disinfection system for Covid-19 and in general for other types of viruses and bacteria conceived and built in our laboratory based on a Fresnel lens concentrator. The demonstration prototype and the first results obtained are briefly described.

Key words. UV Disinfection, Sunlight Concentrators, Fresnel lenses

1. Introduction

It is now quite well known and advertised by all virologists in the world that the influenza virus is easily transmitted by aerosols and a viral shedding in human nasal secretions is reported that can reach up to 10^7 infectious influenza viral particles per milliliter (Couch 1995). Viral shedding in community homes and residential facilities can occur before the onset of symptoms and continue for several days to weeks after symptoms have subsided (Barker et al. 2001). However, epidemiological data on the distribution of influenza as a function of the seasons suggests that environmental factors play a role in the influence of epidemics. The fact that the virus sur-

vives for long periods on surfaces and in the air, the increased infection rate that can be achieved by vigorously sweeping floors indicates that the influenza virus can be readily re-circulated without much loss of infectivity (Loosli et al. 1943). All of this evidence indicates that influenza transmission includes an environmental stage where viruses remain infectious in aerosols or on other environmental surfaces. Studies conducted on the survival of the virus as a function of temperature and humidity have shown that they have a relatively low effect on the inactivation of the influenza virus. Previous studies (Tiller et al. 1983) have shown that the increase in mortality in winter is in largely independent of temperature, humid-

ity or the incidence of other diseases. Although humidity, temperature and other variables can influence the survival of the virus, ultraviolet radiation in sunlight is to be considered as the primary virucidal agent in the environment (Biasin et al. 2021) (Biasin et al. 2021). In the report “Inactivation of Influenza Virus by Solar Radiation” published in the Research and Technology Directorate, the inactivation of viruses due to solar UV radiation in various cities around the world at different times of the year has been calculated. Authors J.L. Sagripanti and C. D Lytle evaluated virus survival after sun exposure by combining the sensitivity of the virus flu to monochromatic radiation at 254 nm obtained in the laboratory with solar radiometry data available for a number of sites in the northern latitudes. These radiometry data were normalized with respect to the action of UV radiation ($\lambda = 254nm$) for the inactivation of the virus previously determined in an experimental data approach. They used $23.5J/m^2$ as the radiation dose to calculate solar virucidal UV fluence (equivalent to 254 nm lambda radiation) for a full day of solar exposure. The maximum daily virucidal solar radiation values calculated for the sites where radiometric data are available are presented in Table 1.

In this calculation both components of solar UV radiation reaching ground level have been considered: the radiation diffused from the sky in general, and the direct ray from the sun which depends on mainly on the solar zenith angle (SZA). Note that during the winter, the level of solar UV radiation needed to inactivate 90% of the influenza A virus in 1 day ($23.5J/m^2$) is only available at latitudes below 30° . On the other hand, in summer all the sites considered have more than $23.5J/m^2$ per day. On a clear sunny day, the two components of solar radiation, direct and indirect (dispersed in the atmosphere), can be roughly equal in intensity. Any area that does not receive total sun exposure, both direct and indirect, for the whole day will obviously have less inactivation of the virus. Less exposure can be caused by cloud cover, dust and chemical pollution, and shadows generated by natural or artificial structures such as trees and build-

Lat °N	Winter Solar UV-B $J/m^2/d$	Fall Solar UV-B $J/m^2/d$	Spring Solar UV-B $J/m^2/d$	Summer Solar UV-B $J/m^2/d$
50	0	38	30	98
48	1	44	25	102
46	1	50	29	108
45	1	50	29	100
44	2	49	31	98
43	4	52	33	105
42	5	64	35	95
40	10	64	40	110
38	10	70	48	110
35	16	91	60	130
33	20	92	70	129
29	30	120	95	162
26	48	129	120	178
20	108	218	216	225

Table 1. Estimated maximum daily solar UV-B radiation (presented as 254 nm equivalent) at different latitudes in the northern hemisphere for different times of the year. Radiometric data from 2005 and 2006..

ings are another cause. The different production of ozone in various places affects the level of UV-B and therefore the level of inactivation of the virus. In any case, the study shows that UV radiation appears to produce a stronger effect than expected. Sagripanti and Lytle conclude that the germicidal impact of solar UV radiation may be several orders of magnitude more relevant than other primary physical factors such as temperature and relative humidity, and that there is an evident correlation between solar radiation and virus inactivation.

2. Solar Irradiance data in the spectral range 150nm - 400nm

Using the Solar Irradiance data in the spectral range 150nm-400nm published in the work (Solar Irradiance from 165 to 400nm in 2008 and UV variations in 3 spectral bands during Solar Cycle 24 (Giese et al. 1976) and plotted in Fig. 1, it can be deduced that the solar irradiance in the range 290-400 nm ranges from about 400 to 1000 mW/m^2nm and therefore:

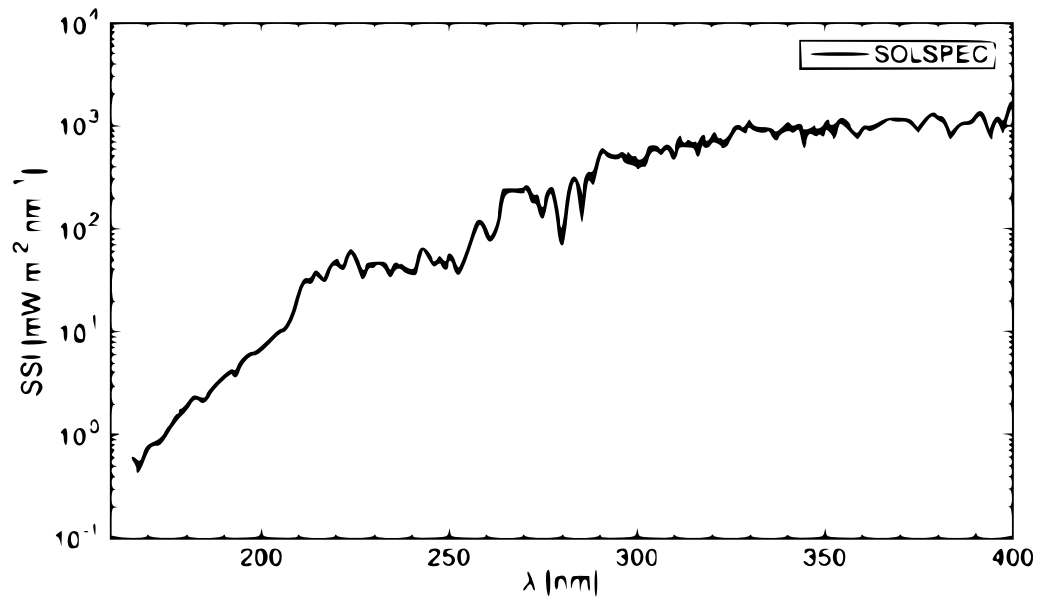


Fig. 1. Solar irradiance in the spectral range 150nm - 400nm during solar cycle 24 SOLA (Ref. 5).

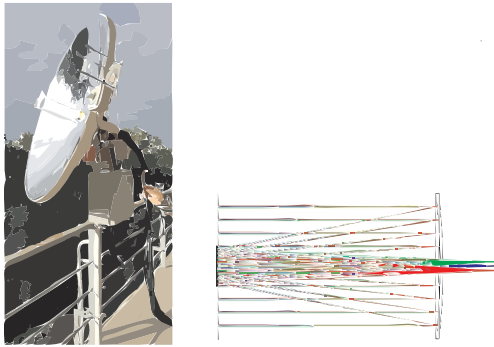


Fig. 2. System with optical concentrator and solar tracking mechanics. In this case, the transport takes place through optical fibers optimized for UV radiation.

1. In the range 290–320 nm (UV-B) the solar irradiance slightly exceeds $400\text{mW}/(\text{m}^2 \times \text{nm})$
2. In the range 320–400 nm (UV-A) the solar irradiance is $1000\text{mW}/(\text{m}^2 \times \text{nm})$

The resulting doses are:

1. In the UV-B band the dose (radiance/s) is approximately $0,4 \times 30 = 12\text{W}/\text{m}^2 \times s$

2. In the UV-A band the dose is approximately $1 \times 80 = 80\text{W}/\text{m}^2 \times s$

If we need a higher dose per unit area and therefore make a disinfection more effective by reducing exposure times, we can use optical concentrators in the two options reflecting mirrors and Fresnel lens transmission systems. In the first case, it is necessary to actively follow the sun with a coelostat, in the second, thanks to the wide field of the lens, the system can be positioned at the geographic latitude angle of the installation, to receive sunlight in a fixed position during all the daylight.

3. Spherical mirror and Fresnel lens concentrators

Fig. 2 shows a prototype of a concentrator spherical mirror system (130 cm diameter corresponding to a collecting area of 1.32 m^2) that uses a secondary mirror that reflects sunlight onto a focal plane where a collection and transport system is placed. In this case a solar tracker is needed and the transport takes place with optical fibers with low absorption in the UV-B and UV-A bands. A solar tracker needs

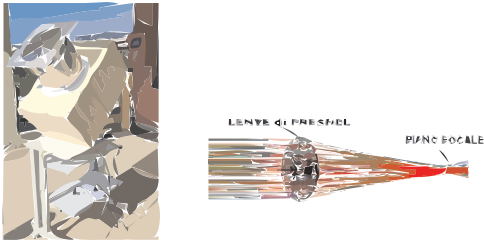


Fig. 3. Fresnel lens concentrator system. In this case, the transport takes place via cylindrical reflecting channels optimized for the reflection of UV radiation.

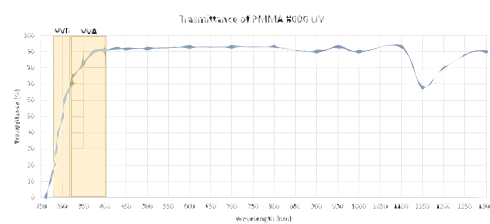


Fig. 4. Fresnel lens manufactured by Nihon Tokushu Kogaku Jushi (NTKJ) Ltd. The lens is made with PMMA # 000 UV transmitting material. In the UV-B band it has a transmittance ranging from about 40% to 75%, while in the UV-A band it has a transmittance ranging from about 70% to 90%.

actuators and electronic controllers, that, apart the mirror, are quite expensive and not easy to install. Furthermore a solar tracker needs maintenance operations.

Fig. 3 shows a prototype demonstrator of a square Fresnel lens concentrator with dimensions of 40x40 cm² and focal length of 60 cm. This lens directly concentrates the sunlight at 60 cm where the collection and transport system is placed. In this case, the transport takes place with cylindrical mirrors optimized for UV-B UV-A radiation.

Fresnel lenses compared to mirror concentrators have the double advantage of being very light and cheaper. The only disadvantage (which leads to slightly higher costs respect to the commercially available) is that they must have the highest possible UV transmittance. For the above mentioned difficulties with the concentrator spherical mirror, we con-



Fig. 5. Sketch of a cylindrical reflecting conduit useful for transporting UV sunlight with high propagation efficiency.

centrated our investigation on Fresnel lenses. Fig. 4 shows the plot of the transmittance as a function of the wavelength of the Fresnel lens manufactured by Nihon Tokushu Kogaku Jushi Ltd (transmitting material PMMA # 000 UV) that was used to realize the demonstrator prototype.

4. Transport of solar radiation through cylindrical reflecting channels

A reflective cylindrical channel or conduit represents an optimal method for transporting the radiation to the area of interest. Fig. 5 shows a sunlight conduit (Ref. 8) and how the light propagates by subsequent reflections.

5. UV Detectors

The system also provides two UV light sensors: one for the UV-B and one for UV-A radiation. These are calibrated in such a way to measure the UV-B power (mW/cm^2) in Volts. A simple Voltmeter can be used to display the voltage level. Eventually these values can be sent to a data acquisition system that can

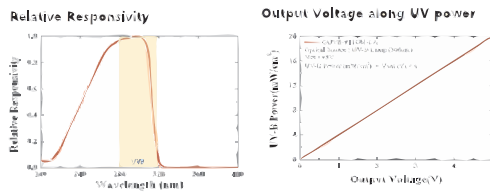


Fig. 6. Relative response of the GUVB-T11GM-LA sensor. Right panel: UV-B power versus voltage.

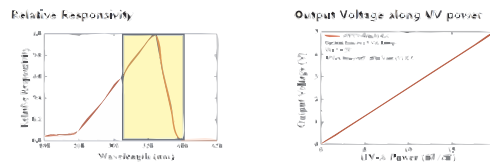


Fig. 7. Left panel: Relative response of the GUVV-S10SM-LA sensor. Right panel: UV-A power versus voltage.

display directly the radiation value and can warn with a visual and audible alarm if the power of UV radiation exceeds a certain set level corresponding to the damage to the skin that can cause some skin cancers, including melanoma. For the radiometric measurement in the UV-B band, the GUVB-T11GM-LA sensor manufactured by Genicom Co., Ltd. is used, which is sensitive only in the 240-320 nm range and is practically “blind” in the other bands. While the GUVV-S10SM-LA manufactured by Genicom Co., Ltd. is used for the radiometric measurement in the UV-A band. The relative response curve of the GUVB-T11GM-LA is shown in the left panel of Figure 6. This sensor is supplied complete with the driving electronics that allows to directly read the power of the UV-B radiation as voltage. The left panel of Fig. 6 shows the calibration curve.

The relative response curve and the calibration curve of the UV-A sensor are shown in Fig. 7.

6. Current status and preliminary results

In order to demonstrate the prototype functionality, we focused in the effect of the radi-

ation concentrated directly on the focal plane of the lens without considering the losses of transportation conduits. In practice, we tried to understand what could be the UV light power available on the focal plane of the lens by concentrating the UV-B and UV-A components of the solar radiation in order to establish how long the exposure had to last to obtain an adequate dose for a complete disinfection. The achieved prototype is shown in the left photo of Fig. 8. While the central photo shows the prototype seen from rear where is clearly evident the light spot created on the wood axis which is placed at the lens focal plane. The photo on the right shows the detail of the light spot, where the UV-B radiation sensor takes place (note the aluminum casing to avoid any burns of the printed circuit that houses it).

We used the prototype in two ways:

1. concentrating the radiation in a light spot of about 1 cm^2 size (see Figure 9);
2. defocusing the light spot on an area of about $2 \times 3 \text{ cm}^2$ (see Fig. 10).

In the case of a very concentrated light spot of 1 cm^2 , the calibrated UV detector with its electronic front-end measures a voltage of about 1.5 Volts that, from the calibration curve (see figure 6) corresponds to 6 mW/cm^2 . While in the case of almost uniform illumination produced on a $2 \times 3 \text{ cm}^2$ spot, the detector front-end measures a voltage of about 0.2 Volt corresponding to 1.5 mW/cm^2 . Considering the notes on disinfection presented by Andrea Bianco in this same volume we can therefore say that:

- a) Disinfection with UV-C radiation occurs with only 4 mJ/cm^2
- b) With UV-B radiation, a 50 times higher dose is required, ie 200 mJ/cm^2

7. Conclusions and future work

We can therefore conclude that if we put an average culture of COVID-19 virus in an area of $2 \times 3 \text{ cm}^2$ with our solar concentrator that produces a radiation of about 1.5 mW/cm^2 , a complete disinfection can be achieved in about 130 seconds. At the time of writing this paper,



Fig. 8. Left photo: Solar concentrator prototype. Central photo: Rear view of the prototype, the light spot created on the wood is clearly evident. Right photo: detail of the light spot, where the GUVB-T11GM-LA detector is placed (note the aluminum casing to avoid any burns of the printed circuit that houses it).

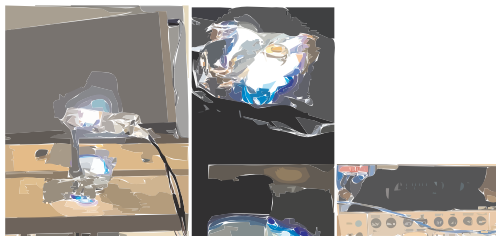


Fig. 9. Left photo: 1 cm^2 light spot intercepted by the UV detector. Central photo: Detail where is seen the UV detector fully illuminated. Right photo: Keithley multi-meter showing the measurement of about 1.5 V corresponding to 6 mW/cm^2 .

we have already designed another much leaner prototype that can be transported to any virology laboratory for possible use in the same laboratory in order to really demonstrate the applicability of this methodology.

References

- Couch, R.B., 1995, Medical Microbiology. University of Texas Medical Branch, Galveston, TX. pp. 1–22
- Barker, J. D. Stevens, and S.F. Bloomfield, 2001, Journal of Applied Microbiology. 91: 7-21
- Loosli, CG, HM Lemon, OH Robertson and E. Appel, 1943, Proc. Soc. Exp.Biol. 53, 205-206
- Tiller, HE, JW Smith and CD Gooch, 1983, Int. J. Epidemiol. 12, 344–352c
- Giese, AC, 1976, Living with Our Sun's Ultraviolet Rays, Chapter 3, pp. 33–34. Plenum Press, New York
- Biasin et al., 2021, Approved for publication on Journal of Photochemistry and Photobiology <https://www.medrxiv.org/content/10.1101/2021.05.28.21257989v1>
- Biasin et al., 2021, Scientific Reports volume 11, Article number: 6260 (2021)



Fig. 10. Left photo: almost uniform light spot of $2 \times 3\text{ cm}^2$. The UV detector is placed in the center. Right photo: Keithley multimeter showing the measurement of about 0.2 V corresponding to about 1.5 mW/cm^2 .